USGS
science for a changing world
U.S. DEPARTMENT OF THE INTERIOR
U.S. GEOLOGICAL SURVEY

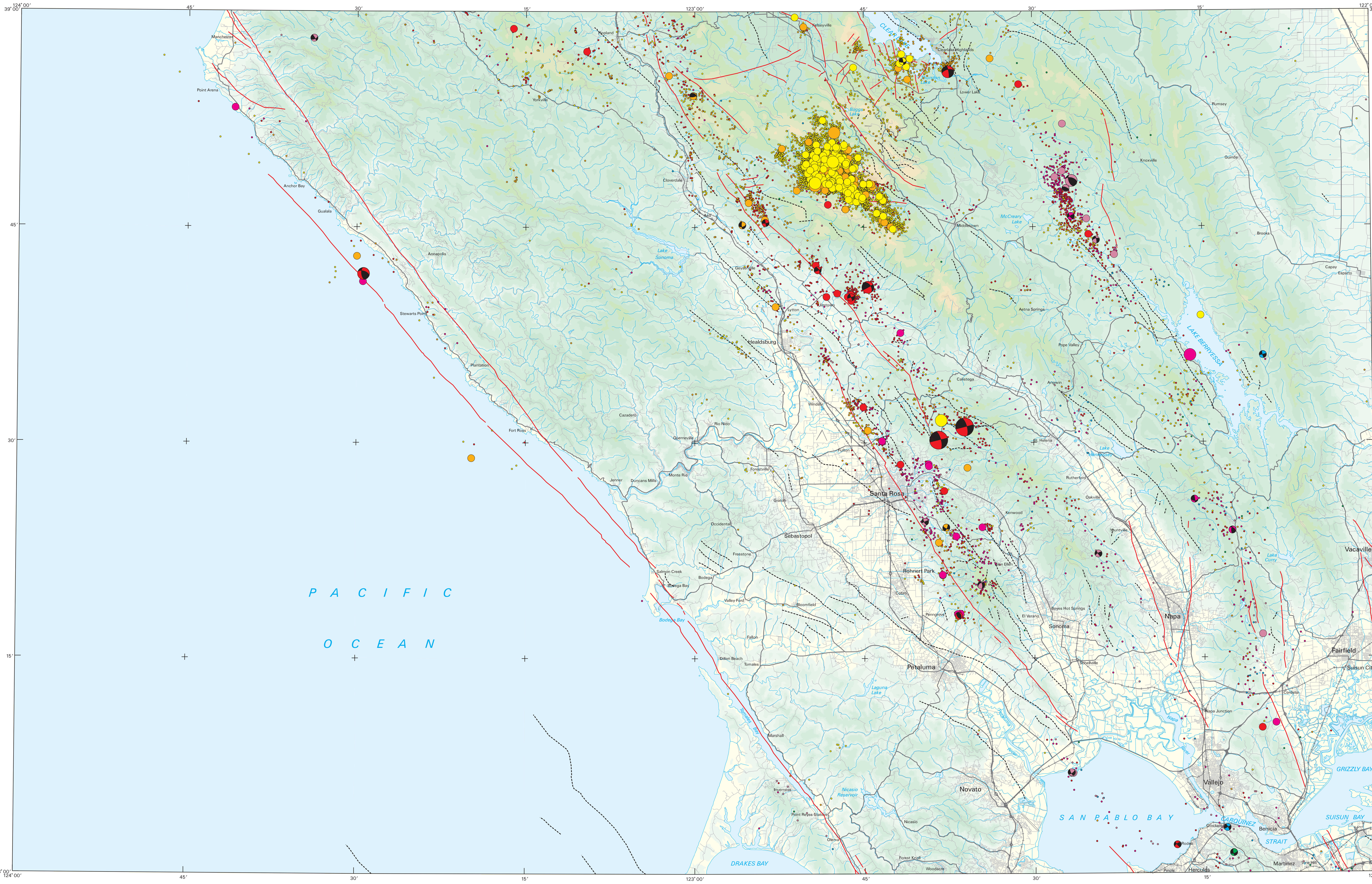

Topography from Defense Mapping Agency 1:250,000-scale Digital Elevation Model (DEM): Santa Rosa (east, west), 1987

Roads and hydrography from U.S. Geological Survey 1:100,000-scale Digital Line Graphs (DLG): Point Arena, 1981; Healdsburg, 1972; Bodega Bay, 1982; Napa, 1983

Geographic names from U.S. Geological Survey 1:100,000-scale published maps: Point Arena, 1981; Healdsburg, 1972; Bodega Bay, 1982; Napa, 1983

Transverse Mercator projection. Longitude of central meridian: 123°W.

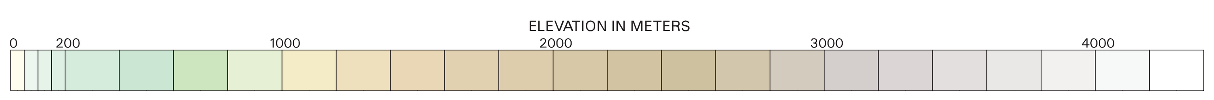

SCALE 1:250 000

5 0 5 10 15 20 25 Statute Miles

5 0 5 10 15 20 25 30 35 Kilometers

Earthquake data compiled by Stephen R. Walter and David H. Oppenheimer, 1996. Digital base map compiled and processed by Jeroen S. Preiss, 1997.

Edited by J.L. Zigler. Digital production by Stephen R. Walter, Jeroen S. Preiss, and David H. Oppenheimer, with technical assistance from Taryn A. Lindquist.

Manuscript approved for publication May 15, 2002.

EXPLANATION

(Symbols shown on map are a combination of magnitude, depth, and focal mechanism (see figure 1) parameters)

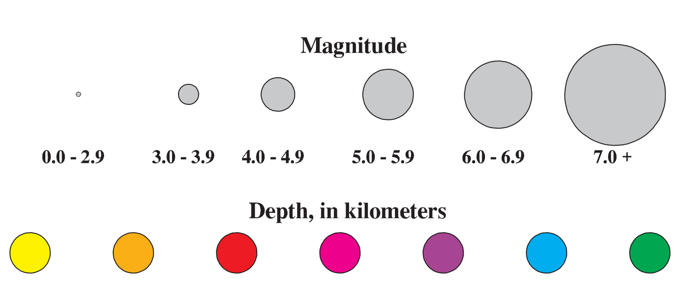

Faults

(Fault traces were digitized at 1:750,000 (Jennings, 1994) and may be mislocated by as much as 0.8 km (0.5 mi) when plotted on this map at 1:250,000. Fault traces are not intended for engineering or land-use purposes.)

Late Quaternary (displacement <700,000 yr)

Early Quaternary (displacement <1,600,000 yr)

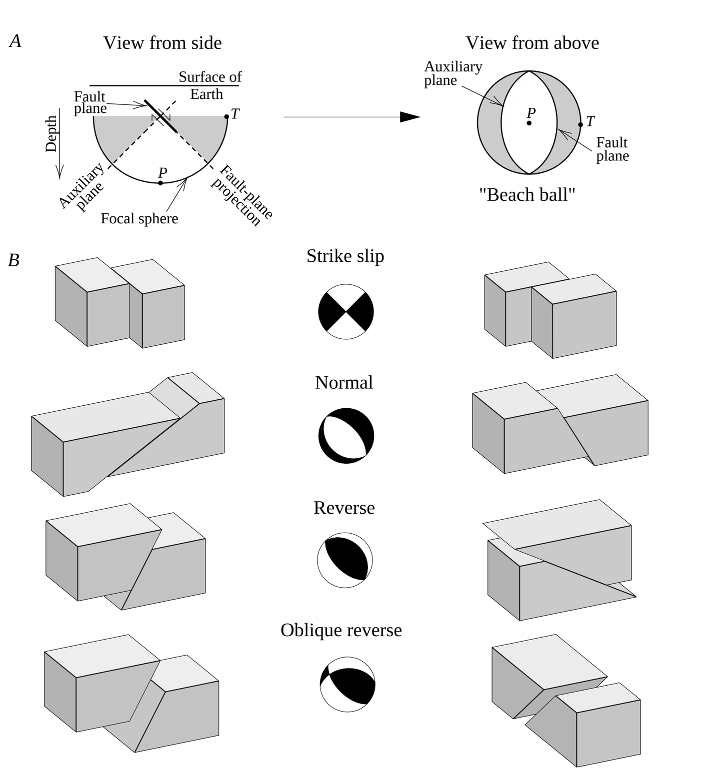

Figure 1. Schematic diagram of a focal mechanism.

Seismologists refer to the direction of slip in an earthquake and the orientation of the fault on which it occurs as the *focal mechanism*. They use information from seismograms to calculate the focal mechanism and typically display it on maps as a “beach ball” symbol (*A*). This symbol is the projection on a horizontal plane of the lower half of an imaginary, spherical shell (*focal sphere*) surrounding the earthquake source. A line is scribed where the fault plane intersects the shell. The stress-field orientation at the time of rupture governs the direction of slip on the fault plane; the beach ball depicts this stress orientation through shading. The black quadrants contain the tension axis (*T*), which reflects the minimum stress direction, and the white (or colored on the map) quadrants contain the pressure axis (*P*), which reflects the maximum stress direction.

For mechanisms calculated from the first-motion direction of seismograms, there is an ambiguity in identifying the fault plane on which slip occurred from the orthogonal, mathematically equivalent, *auxiliary* plane. We illustrate this ambiguity with four examples (*B*). The block diagrams adjacent to each focal mechanism illustrate the two possible types of fault motion that the focal mechanism could represent. Note that the view angle is 30° to the left of and above each diagram. The ambiguity may be resolved by comparing the two fault-plane orientations to the alignment of small earthquakes and aftershocks shown in map and cross-section views. The first three examples describe fault motion that is purely horizontal (*strike slip*) or vertical (*normal* or *reverse*). The *oblique-reverse* mechanism illustrates that slip may also have components of horizontal and vertical motion.

INDEX TO 1° × 2° QUADRANGLES SHOWING MAP AREA (BOLD BOX)

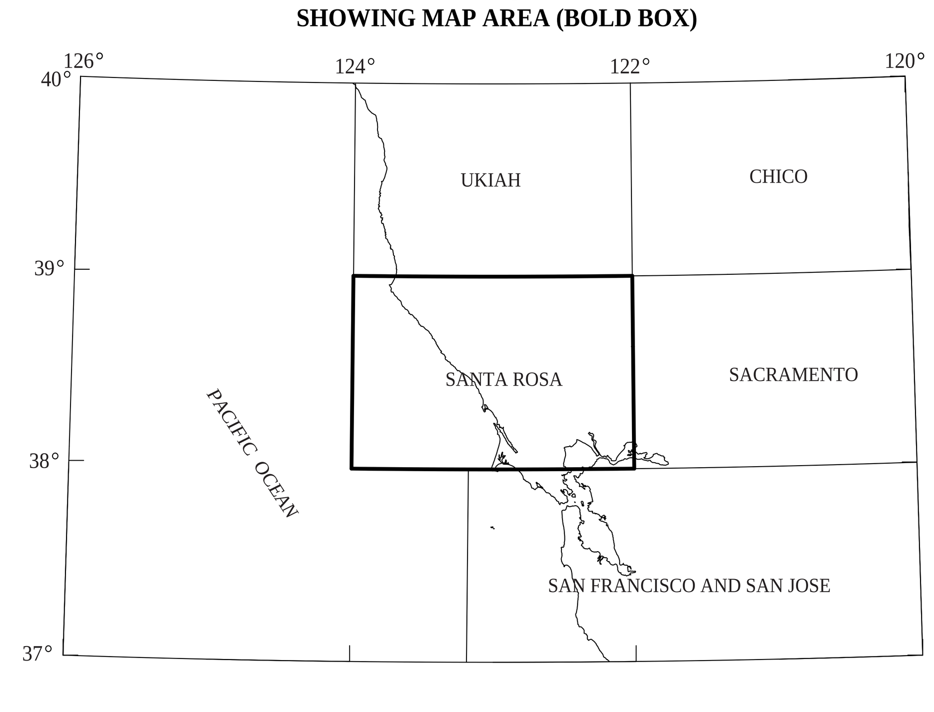

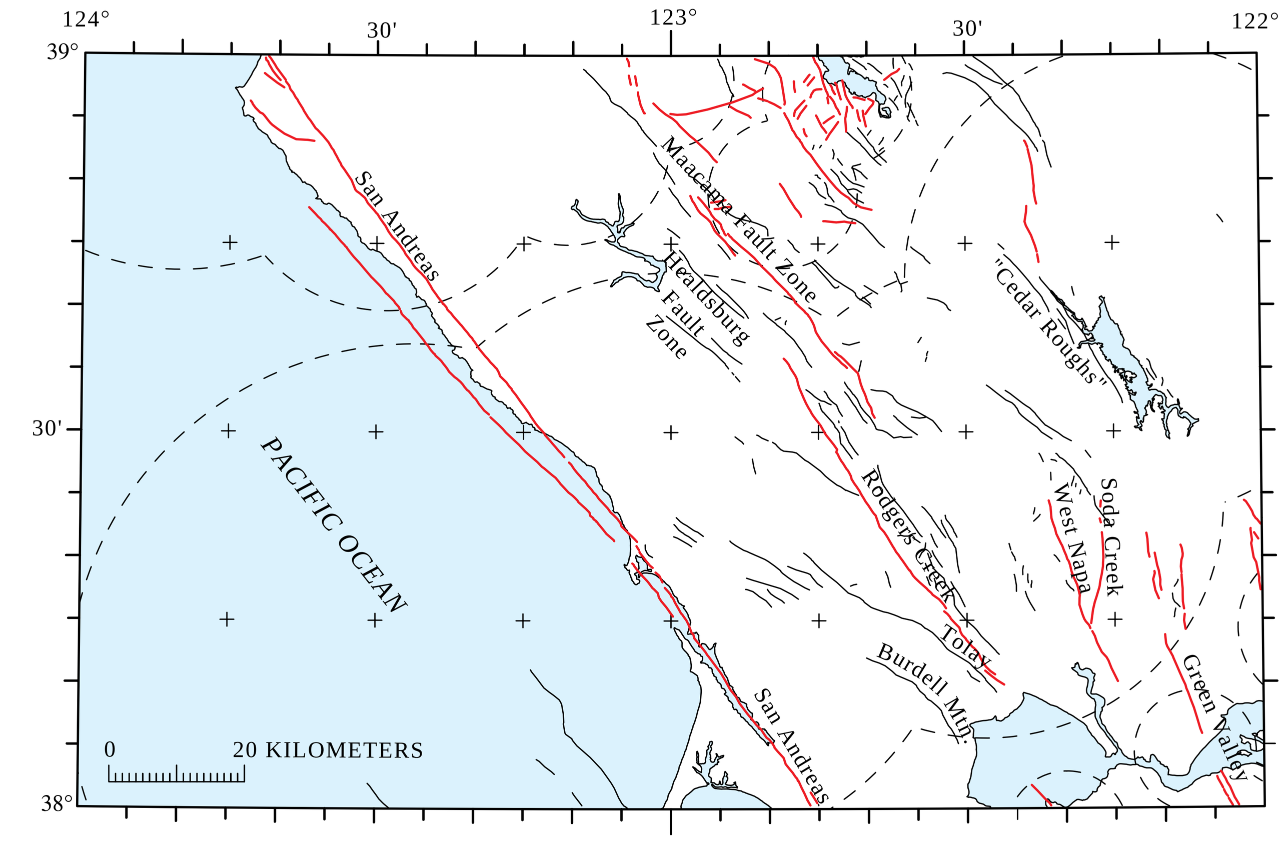

Figure 2. Principal fault systems and velocity-model boundaries.

This figure shows geologically mapped faults of Quaternary age (Jennings, 1994) in the Santa Rosa quadrangle and the boundaries of velocity models used to locate the earthquakes. Red faults exhibit displacement within the last 700,000 years. Black faults exhibit displacement sometime in the last 1,600,000 years. Faults may also exist in this region that have no surface expression but are capable of producing significant earthquakes.

Each earthquake location was calculated using the computer program HYPOINVERSE (Klein, 1989) from one of six crustal velocity models specific to the region where the earthquake occurred. Multiple velocity models improve the accuracy of the earthquake locations by partly accounting for lateral variations in velocity within the crust. The boundaries of the velocity regions, which extend beyond the borders of this map, are indicated with dashed curved lines. For models that encompass large regions, the model boundaries are constructed by a series of overlapping circles. The velocity models vary with depth and have associated station traveltime corrections (Oppenheimer and others, 1993). Events occurring between specified velocity regions are located with an interpolation of the closest two or three models.

MAP A - SEISMICITY

INTRODUCTION

This map set depicts several aspects of recorded seismicity that occurred from 1967 through 1995 within the Santa Rosa, California quadrangle. Map A on this sheet and the related cross sections shown on sheets 2 and 3 illustrate the locations, depths, and magnitudes of earthquakes. On maps A and D we also plot representative focal mechanisms (see fig. 1) to indicate the fault orientation and direction of motion on many faults. On map B and on the cross sections of sheets 2 and 3 we identify the most significant temporal clusters of earthquakes to illustrate the time-dependent properties of earthquake occurrence. Maps C and D are enlarged views of the seismicity at The Geysers geothermal area. Map C shows the time-dependent relation between the inception of geothermal power production and the occurrence of earthquake activity.

In the following discussion we make a subtle inference about the relation of seismicity to faults mapped at the surface. Where concentrations of earthquakes locate beneath mapped faults, we infer that the seismicity defines the subsurface orientation of these faults. Even though some concentrations of earthquakes do not underlie mapped faults, we also infer that these concentrations represent active, but as yet unnamed faults. Earthquakes also occur as isolated events beneath mapped faults and throughout the region.

PRESENTATION OF SEISMICITY

The 31,943 earthquakes shown on map A were recorded by the Northern California Seismic Network, which is operated by the U.S. Geological Survey. The size and color of each symbol on the map depicts the earthquake magnitude and depth interval, respectively (see Explanation). The symbol size and order in which the symbol is plotted greatly affects the presentation of information. Because we plot the earthquake symbols before the focal mechanisms, previously plotted earthquakes may be obscured. We plot the earthquakes by the magnitude interval shown in the Explanation ($M < 3.0$ first, then largest interval to smallest interval), and within each magnitude interval we plot events by depth (deepest to shallowest). We then plot the focal mechanisms of large earthquakes before the mechanisms of smaller earthquakes. This plot order may obscure deeper and smaller earthquakes in map view, particularly when they occur within dense concentrations as at The Geysers, but the cross sections on sheets 2 and 3 reveal this information. Focal mechanisms at The Geysers are shown in more detail on map D.

We show the M_L (Local) magnitude, if available, and otherwise use the M_D (coda duration) magnitude. No minimum magnitude selection criteria were imposed. We have attempted to remove all explosions from the data shown on these maps, but some shallow, isolated events may not be earthquakes. Most earthquakes shown on these maps have location parameters that meet the following criteria: horizontal location uncertainty < 2.5 km; depth uncertainty < 5.0 km; 8 or more *P*-wave readings; the maximum azimuthal gap <180° (the angle defined by azimuthally adjacent seismic stations used to locate the earthquake and the epicenter) ; solution traveltime residual $RMS < 0.3$ sec. However, we have increased the gap criteria to 270° for 75 earthquakes occurring offshore and near the coastline. During the interval 1969 - 1995 we located only 17 earthquakes, all with a $M < 3.0$, in the Pacific Ocean west of a line connecting Pt. Reyes and the northwest corner of the map (latitude 39°, longitude -124°). We do not show these events because the accuracy of the locations is very poor. The above selection criteria do not eliminate systematic location errors. For example, if the location error systematically increases as a function of hypocentral depth, a vertical fault may appear to have a slight dip in cross section. Systematic errors may result from our use of one-dimensional velocity models to locate earthquakes in a crust where the velocity varies in three dimensions (fig. 2).

The “beach ball” symbols depict double-couple focal mechanisms (see fig. 1) calculated using the method of Reasenberg and Oppenheimer (1985). Because the calculated mechanisms are based on compressional wave (*P*) first-motion readings, they represent the fault orientation and slip direction only at the point of rupture initiation. The 32 representative $M > 3$ earthquakes shown on map A have a minimum of 30 first-motion readings. The size and color of the focal-mechanism symbols represent the same information as shown by other earthquake symbols. Typically, the slip plane is distinguished from the auxiliary plane by comparing alignments in seismicity or the mapped orientation of faults at the surface to the mechanism. As discussed below, in this quadrangle the seismicity appears to locate adjacent to some of the mapped faults, like the Rodgers Creek or Green Valley, rather than directly on the fault. Thus, designation of the slip plane may be uncertain.

SEISMICITY OVERVIEW

Earthquakes occurring during 1969–1995 locate on several fault systems that traverse the Santa Rosa quadrangle. An interesting observation is the near absence of seismicity on the San Andreas fault (fig. 2). During the *M*7.9 1906 earthquake the San Andreas fault slipped about 6 m at Pt. Reyes (Lawson, 1908), and undoubtedly thousands of aftershocks occurred (*e.g.*, the 1989 Loma Prieta, California, *M* 7.0 earthquake had more than 7000 aftershocks in the subsequent two year period). Unfortunately, the record of seismic activity for the 1906 earthquake was not recorded because there were no functional seismic networks at that time. The disparity in the numbers of earthquakes on the San Andreas fault during the interval shown on this map and the number of aftershocks that likely followed the 1906 quake illustrates an important point - earthquake activity during this time interval should not be considered representative of the long-term seismicity of this region. Most of the contemporary earthquakes near the San Andreas fault locate about 5 km west of the fault. Because the nearest seismic stations are 10-20 km from these earthquakes and there are no seismic stations to the west of these earthquakes, it is difficult to obtain accurate locations or depths. Hence, they may be systematically mislocated and instead be occurring on the fault.

Scattered seismicity occurred along the Rodgers Creek-Healdsburg-Maacama fault system (fig. 2). Like the San Andreas fault, the Rodgers Creek fault has almost no seismicity south of the town of Penngrove even though Budding *et al.* (1991) demonstrate that this segment of the fault is active and capable of rupturing in a *M*7 earthquake. North of Penngrove the seismicity follows the Rodgers Creek fault over a zone several kilometers wide, ending near the Healdsburg. The few focal mechanisms available indicate right-lateral slip on a near-vertical fault. Likewise, cross-section F on sheet 2 suggests that the fault is near vertical. The Maacama fault, whose orientation is parallel to and east of the Rodgers Creek fault, extends from Santa Rosa northwest past Hopland. The style of seismicity on the Maacama and Rodgers Creek faults are quite similar. Focal mechanisms also indicate right-lateral slip on a near vertical fault, and the earthquakes occur over a zone several kilometers wide. The scatter in earthquake locations along these two faults exceeds the formal uncertainty in the computed locations. Consequently, these earthquakes may not occur directly on the Rodgers Creek or Maacama fault, but rather on minor, subsidiary faults. The seismicity on the San Francisco peninsula in the quadrangle immediately to the south is quite similar, where minor seismicity apparently occurs on faults and fractures adjacent to the San Andreas fault (Walter *et al.*, 1997).

The region between the Maacama and Rodgers Creek faults is the site of the “Santa Rosa earthquakes”. On October 1, 1969, a *M*5.6 was followed 1 hour, 23 minutes later by a *M*5.7 quake. Because so few seismic stations were in operation in 1969, the distance to the nearest station is greater than 50 km. Consequently, the earthquake depths and locations are poorly known compared to locations of earthquakes recorded after 1975. Wong and Bott (1995) relocated the Santa Rosa mainshocks with a procedure that differs from that used here. The mainshock locations shown here are about 5 km northeast of those reported by Wong and Bott. Although our computed horizontal location uncertainties are less than 3 km for these earthquakes, the discrepancy between our results and those reported by Wong and Bott suggest that the real location uncertainty may be larger. The locations from Wong and Bott are close to the intersection of the Healdsburg and Rodgers Creek faults, whereas those shown here are near the southwest terminus of the Maacama fault zone. Their mechanisms indicate vertical, right-lateral, strike-slip motion on a north-northwest-striking fault. Like the earthquake locations, the accuracy of the focal mechanisms for these two quakes is quite poor. Focal mechanisms for other earthquakes occurring on this fault system, however, also indicate similar fault motion. The Santa Rosa mainshocks may have occurred on the northwest-oriented Healdsburg, Rodgers Creek, or Maacama faults, but Wong and Bott note that they may also have ruptured an unmapped, left-lateral, northeast striking cross-fault, similar to the cross-fault linking the Calaveras and Concord faults near Alamo, California which ruptured in 1990 (Walter *et al*., 1997).

Minor earthquake activity along the Green Valley-Cedar Roughs fault system (fig. 2) indicates this fault system is also active (Wong, 1990). The scatter in the epicentral locations as well as the scatter shown in cross-section F (sheet 2, map B) suggests that the earthquakes may be occurring on small subsidiary faults adjacent to a near-vertical fault that is currently quiescent. The few available mechanisms indicate right-lateral, strike-slip motion on north-to-northwest striking faults. Earthquakes also occur northwest of the mapped portion of the Cedar Roughs fault and west of the Hunting Creek fault (cluster 12, map B), which suggests that the Green Valley-Cedar Roughs fault system continues to the northwest in a linear trend, even though the fault is not mapped at the surface. However, a *M*3.1 quake in this cluster exhibits a significant component of reverse motion on a plane parallel to the trend in seismicity. This event locates about 2 km northeast of the trend of seismicity associated with cluster 12, again suggesting slip on a fault adjacent to the Green Valley-Cedar Roughs fault.

The Geysers geothermal area was the most seismically active region during this time interval. The earthquake hypocenters do not occur on faults mapped at the surface, but occur in a volume coincident with the region of geothermal steam withdrawal and fluid reinjection. Expanded maps, cross-sections, and discussions of The Geysers seismicity are provided on sheet 3.

Finally, seismicity occurs immediately southeast of Clear Lake (Eberhart-Phillips, 1988) in an area where volcanism occurred about 10,000 years ago (Donnelly-Nolan *et al.*, 1981). The earthquakes do not image any single fault, but appear to occur on the numerous, relatively small, faults shown on map A and figure 2. Identification of the slip plane from the two focal mechanisms in this region is ambiguous (see discussion in fig. 1), but the mechanisms indicate vertical faults with strike-slip motion.

ACKNOWLEDGMENTS

We thank Robert McLaughlin and Richard Blakely for their careful reviews.

REFERENCES CITED

Budding, K.E., Schwartz, D.P., and Oppenheimer, D.H., 1991, Slip rate, earthquake recurrence, and seismogenic potential of the Rodgers Creek Fault zone, northern California: Initial results: Geophysical Research Letters, v. 18, 447-450.

Donnelly-Nolan, J.M., Hearn, B.C., Jr., Curtis, G.H., and Drake, R.E., 1981, Geochronology and evolution of the Clear Lake Volcanics, *in* Research in the Geysers-Clear Lake geothermal area, northern California, McLaughlin, R.J., and Donnelly-Nolan, J.M., editors, p. 47-60, U.S. Geological Survey Professional Paper 1141.

Eberhart-Phillips, D., 1988, Seismicity in the Clear Lake area, California, 1975-1983: *in* Cores from Clear Lake: Lake Quaternary Record of Climate, Tectonics and Lake Sedimentation in the Northern California Coast Ranges, J. Sims, editor, p. 195-206, Geological Society of America Special Paper 214.

Eberhart-Phillips, D., and Oppenheimer, D.H., 1984, Induced seismicity in The Geysers geothermal area, California: Journal of Geophysical Research, v. 89, p. 1191-1207.

Jennings, C.W., 1994, Fault activity map of California and adjacent areas: California Division of Mines and Geology, California Geologic Data Map Series, no. 6, scale 1:750,000, 1 sheet.

Klein, F.W., 1989, User’s guide to HYPOINVERSE, a program for VAX computers to solve for earthquake locations and magnitudes: U.S. Geological Survey Open-File Report 89–314, 61 p.

Lawson, A.C., chairman, 1908, The California Earthquake of April 18, 1906: Report of the State Earthquake Investigation Commission: Carnegie Institution of Washington Publication 87, 2v.

Oppenheimer, D., Klein, F., Eaton, J., and Lester, F., 1993, The Northern California Seismic Network Bulletin January–December 1992: U.S. Geological Survey Open-File Report 93–578, 45 p.

Oppenheimer, D.H., 1986, Extensional tectonics at The Geysers Geothermal Area, California: Journal of Geophysical Research, v. 91, p. 11,463-11476.

Reasenberg, P., 1985, Second-order moment of central California seismicity: Journal of Geophysical Research, v. 90, p. 5479–5495.

Reasenberg, P.A., and Oppenheimer, D., 1985, FPFIT, FPPLOT, and FPPAGE: Fortran computer programs for calculating and displaying earthquake fault-plane solutions: U.S. Geological Survey Open-File Report 85–739, 109 p.

Wagner, D.L., and Bortugno, E.J., 1982, Map showing recency of faulting, Santa Rosa quadrangle, California, 1:250,000: California Division of Mines and Geology, Regional Geologic Map Series, no. 2A, 5 sheets.

Walter, S.R., Oppenheimer, D.H., and Mandel, R.I., 1997, Seismicity map of the San Francisco and San Jose 1° × 2° quadrangles, California for the Period 1967-1993: U.S. Geological Survey Miscellaneous Investigations Series Map I-2580, 1:250,000, 3 sheets.

Wong, I.G., 1990, Seismotectonics of the Coast Ranges in the vicinity of Lake Berryessa, northern California: Bulletin Seismological Society of America, v. 80, p. 935-950.

Wong, I.G., and Bott, J.D.J., 1995, A new look back at the 1969 Santa Rosa, California, earthquakes: Bulletin Seismological Society of America, v. 73, p. 334-341.

OTHER REFERENCES

Eberhart-Phillips, D., 1986, Three-dimensional velocity structure in northern California Coast Ranges from inversion of local earthquake arrival times, Bulletin Seismological Society of America, 76, 1025-1052.

Julian, B.R., Ross, A., Foulger, G.R., and Evans, J.R., 1996, Three-dimensional seismic image of a geothermal reservoir: The Geysers, California, Geophysical Research Letters, 23, 685-688.

McLaughlin, R.J., and Donnelly-Nolan, J.M., editors, 1981, Research in the Geysers-Clear Lake geothermal area, northern California, U.S. Geological Survey Professional Paper 1141.

Stanley, W.D., and Blakely, R.J., 1995, The Geysers-Clear Lake geothermal area, California -- An updated geophysical perspective of heat sources: Geothermics, v. 24, p 187-221.

Stone, C., 1992, editor, Monograph on The Geysers geothermal field: Geothermal Resources Council Transactions, Special Report 17.

Zucca, J.J., Hutchings, L.J., and Kasameyer, P.W., 1993, Seismic velocity and attenuation structure of the Geysers geothermal field, CA: Geothermics, v. 23, p. 111-126.

Wallace, R.E., editor, 1990, The San Andreas fault system, California: U.S. Geological Survey Professional Paper 1515.

SEISMICITY MAPS OF THE SANTA ROSA 1° × 2° QUADRANGLE, CALIFORNIA FOR THE PERIOD 1969-1995

by

Jeroen S. Preiss, Stephen R. Walter, and David H. Oppenheimer

2002

The publication also includes digital versions of the map sheets, which are available on the World Wide Web at: http://geopubs.wr.usgs.gov/open-file/of02-209.